J. Fluid Mech. (1981), *vol.* 112, *pp.* 467–474
Printed in Great Britain

Finite-amplitude stability of axisymmetric pipe flow

By ANTHONY T. PATERA AND STEVEN A. ORSZAG

Department of Mathematics, Massachusetts Institute of Technology, Cambridge, Massachusetts 02139

(Received 18 September 1980 and in revised form 20 January 1981)

The stability of pipe flow to axisymmetric disturbances is studied by direct numerical simulation of the incompressible Navier-Stokes equations. There is no evidence of finite-amplitude equilibria at any of the wavenumber/Reynolds number combinations investigated, with all perturbations decaying on a time scale much shorter than the diffusive (viscous) time scale. In particular, decay is obtained where amplitude-expansion perturbation techniques predict equilibria, indicating that these methods are not valid away from the neutral curve of linear stability theory.

1. Introduction

It is generally accepted that pipe Poiseuille flow (Hagen–Poiseuille flow) is linearly stable to all disturbances (both axisymmetric and non-axisymmetric) at all Reynolds numbers (Sexl 1927; Lessen, Sadler & Lui 1968; Davey & Drazin 1969; Metcalfe & Orszag 1973; Salwen, Cotton & Grosch 1980). Therefore, the explanation of the observed transition to turbulence in this flow requires finite-amplitude instabilities.

Finite-amplitude stability analyses of pipe flow have so far been restricted to axisymmetric disturbances (Davey & Nguyen 1971) and even these results are not without controversy (Itoh 1977; Davey 1978). In this paper, we use spectral methods to investigate numerically the behaviour of finite-amplitude axisymmetric disturbances in pressure-driven pipe flow. The basic question concerns the existence of finite-amplitude equilibrium states of this flow. If such states do not exist then pipe flow is stable to all axisymmetric disturbances. Available finite-amplitude analyses predict equilibria, but they are in disagreement over both results and methodology.

2. Numerical methods

The axisymmetric incompressible Navier–Stokes equations are, in rotation form,

$$\frac{\partial u}{\partial t} = -\frac{\partial \Pi}{\partial x} + \frac{4}{R} + v\omega + \frac{1}{R}\left(D^2 + \frac{\partial^2}{\partial x^2}\right)u, \tag{1}$$

$$\frac{\partial v}{\partial t} = -\frac{\partial \Pi}{\partial r} - u\omega + \frac{1}{R}\left(D^2 - \frac{1}{r^2} + \frac{\partial^2}{\partial x^2}\right)v, \tag{2}$$

$$\frac{\partial}{\partial x}(ru) + \frac{\partial}{\partial r}(rv) = 0, \tag{3}$$

where u and v are the velocities in the x and r directions, respectively,

$$D^2 = r^{-1}(\partial/\partial r)\,(r\partial/\partial r),$$

and $\omega = \partial v/\partial x - \partial u/\partial r$ is the azimuthal vorticity. The boundary conditions on the velocities are

$$u, v/r \text{ bounded} \quad (r = 0), \quad u, v = 0 \quad (r = 1); \tag{4}$$

R is the Reynolds number based on pipe radius and centre-line velocity. The constant pressure gradient term is assumed to be that of the laminar flow, namely $4/R$, and Π is the disturbance pressure head.

We discuss briefly below four features of our numerical methods: spectral representation; time-stepping; operator inversion; and initial conditions. The major difference between the present pipe-flow calculations and our plane channel-flow simulations (Orszag & Kells 1980; Patera & Orszag 1980) is that variable-coefficient equations must now be solved implicitly, whereas in planar geometry only constant coefficient equations require implicit solution.

The velocities are expanded as

$$u(x,r,t) = \sum_{|n|\leqslant N} \sum_{p=0}^{P} \tilde{u}(n,p,t)\, e^{i\alpha n x} T_{2p}(r), \tag{5}$$

$$v(x,r,t) = \sum_{|n|< N} \sum_{p=0}^{P} \tilde{v}(n,p,t)\, e^{i\alpha n x} T_{2p+1}(r), \tag{6}$$

where the Chebyshev polynomials $T_q(r)$ are defined by

$$T_q(\cos\theta) = \cos q\theta.$$

The even (odd) nature of $u(v)$ follows naturally from the axisymmetry of the problem. Boundedness at the origin is then automatically imposed. Periodic boundary conditions are applied in x with periodicity interval $2\pi/\alpha$.

A fractional time-stepping method (Orszag & Kells 1980) is used, each full step consisting of (i) a nonlinear step, (ii) a pressure step, and (iii) a viscous dissipation step. For the first fractional step a second-order Adams–Bashforth method is used:

$$\hat{u}^{n+1} = u^n + \Delta t(\tfrac{3}{2}v^n\omega^n - \tfrac{1}{2}v^{n-1}\omega^{n-1} + 4/R),$$
$$\hat{v}^{n+1} = v^n + \Delta t(-\tfrac{3}{2}u^n\omega^n + \tfrac{1}{2}u^{n-1}\omega^{n-1}),$$

where the superscript refers to time step. The nonlinear terms are calculated efficiently using transform methods and collocation (pseudospectral) techniques (Gottlieb & Orszag 1977). Products are evaluated in physical space while derivatives are calculated in spectral space. Transformations between the two representations are done using extensions of the fast Fourier transform algorithm. In the remainder of this section it is assumed that the velocities are in mixed representation, Fourier in x but physical in r. The axial wavenumber of a Fourier mode will be denoted by γ.

Next, incompressibility is imposed with the pressure step

$$\hat{\hat{u}}^{n+1} = \hat{u}^{n+1} - i\gamma\Delta t\Pi^* \quad (r < 1), \tag{7}$$

$$\hat{\hat{v}}^{n+1} = \hat{v}^{n+1} - \Delta t\frac{\partial \Pi^*}{\partial r} \quad (r < 1), \tag{8}$$

$$i\gamma r\hat{\hat{u}}^{n+1} + \frac{\partial}{\partial r}(r\hat{\hat{v}}^{n+1}) = 0 \quad (r \leqslant 1), \tag{9}$$

$$\hat{\hat{v}}^{n+1} = 0 \quad (r = 1), \tag{10}$$

where we write Π^* rather than Π to indicate that the pressure obtained here is an intermediate result. Equations (7)–(10) can be combined to give a single equation for Π^*,

$$(D^2-\gamma^2)\,\pi^* = i\gamma\hat{u}^{n+1}+\frac{1}{r}\frac{\partial}{\partial r}(r\hat{v}^{n+1}) \quad (r<1), \tag{11}$$

$$\frac{\partial \Pi^*}{\partial r} = 0 \quad (r=1). \tag{12}$$

Note that Π^* is expanded in an even series of Chebyshev polynomials like (5). The solution of (11)–(12) is discussed below.

In the final fractional step, viscous effects are included using the Euler backward scheme

$$u^{n+1} = \hat{\hat{u}}^{n+1}+\frac{\Delta t}{R}(D^2-\gamma^2)\,u^{n+1} \quad (r<1), \tag{13}$$

$$u^{n+1} = 0 \quad (r=1), \tag{14}$$

$$v^{n+1} = \hat{\hat{v}}^{n+1}+\frac{\Delta t}{R}\left(D^2-\frac{1}{r^2}-\gamma^2\right)v^{n+1} \quad (r<1), \tag{15}$$

$$v^{n+1} = 0 \quad (r=1). \tag{16}$$

The overall scheme is only first-order accurate in time because the viscous and pressure operators do not commute. Higher-order accuracy in time may be obtained by extrapolation methods.

The implicit parts of the procedure given above all involve solution of an equation of the form

$$(L-\beta^2)\,\phi = f \quad (r<1), \tag{17}$$

$$a\phi+b\frac{\partial\phi}{\partial r} = 0 \quad (r=1), \tag{18}$$

for each Fourier mode, where L is a second-order (Laplacian) operator in r, β^2 depends only on the x-Fourier index (not r), and a and b are constants independent of Fourier mode. We discuss briefly here the discretization of L and the method of inversion. For planar geometries L can be written as a tri-diagonal system using a Chebyshev tau-method (Orszag & Kells 1980). This system can then be inverted in $O(P)$ operations for each x-Fourier mode. The curvature terms introduced by the cylindrical geometry destroy the tridiagonal property of the tau-method matrix, and collocation then becomes more attractive due to the ease with which variable coefficient problems can be handled.

To solve the full matrix equations resulting from the collocation approximation of (17)–(18), an eigenfunction solver is used that reduces the operation count from $O(P^3)$ to $O(P^2)$ while only requiring the storage of one $P\times P$ matrix for given (L, a, b). More precisely, we diagonalize the collocation approximation to L as

$$L = \Psi^{-1}\Lambda\Psi.$$

The solution to (17)–(18) can then be written as

$$\phi = \Psi^{-1}(\Lambda-\beta^2 I)^{-1}\Psi f.$$

The diagonalization (independent of Fourier mode) is done in a pre-processing stage.

	Wall Mode	Centre Mode
R	1600	500
α	5·8	6·2
Re ω	1·5849	5·8852
Im ω	−0·5396	−0·3917
Perturbation energy	1×10^{-10}	1×10^{-10}
spatial resolution $(2N\times(P+1))$	8×33	8×17
Δt	0·005	0·01
Final time, T	10	10
Computed Re ω	1·5836	5·9146
Computed Im ω	−0·5410	−0·3876

TABLE 1. Behaviour of linear modes

Finally, the initial conditions for the runs presented here are of the form

$$\mathbf{v}(x,r,t=0) = (1-r^2)\,\mathbf{x}+A\,\mathbf{v}_L(x,r)$$

where $\mathbf{v} = (u,v)$ and $\mathbf{v}_L$ is an eigenfunction of the fourth-order linear stability equation obtained from (1)–(3) by assuming a solution of the form

$$\mathbf{v} = (1-r^2)\,\mathbf{x}+\epsilon\boldsymbol{\psi}(r)\,e^{i(x-\omega t)\alpha}$$

and linearizing with respect to ϵ. The magnitude of the perturbation is characterized by its energy relative to that of the unperturbed flow:

$$E = 12\int_0^1 (u^2+v^2)\,r\,dr. \tag{19}$$

The details of the linear problem are well-documented (Lessen *et al.* 1968; Davey & Drazin 1969; Salwen *et al.* 1980) and will not be discussed here. The numerical procedure used to determine the eigenvalue ω and eigenfunction $\psi(r)$ for given R, α is similar to that described by Orszag (1971) for planar geometries, except that collocation rather than the tau-method is used.

3. Results

Before investigating finite-amplitude behaviour it is necessary to confirm that the direct simulation gives decay rates and phase velocities in agreement with those predicted by linear theory. The results of two such tests are summarized in table 1, where it is seen that the code adequately resolves both centre and wall modes at modest time steps (even without using extrapolation methods to reduce the first-orders error in time).

The results of linear theory can also be used to test whether interactions between a primary mode and its harmonic are accurately simulated. For pipe flow, a centre mode with wavenumber α nearly resonates with its harmonic in the sense that the phase speed of the mode with wavenumber 2α is very close to that of the primary. If one assumes they resonate exactly (i.e. $\omega_{2r} = 2\omega_{1r}$), the harmonic will obey a forced amplitude equation of the form

$$\frac{\partial A_2}{\partial t} = \omega_{2i}\,A_2+O(A_1^2)\,e^{2\omega_{1i}t}$$

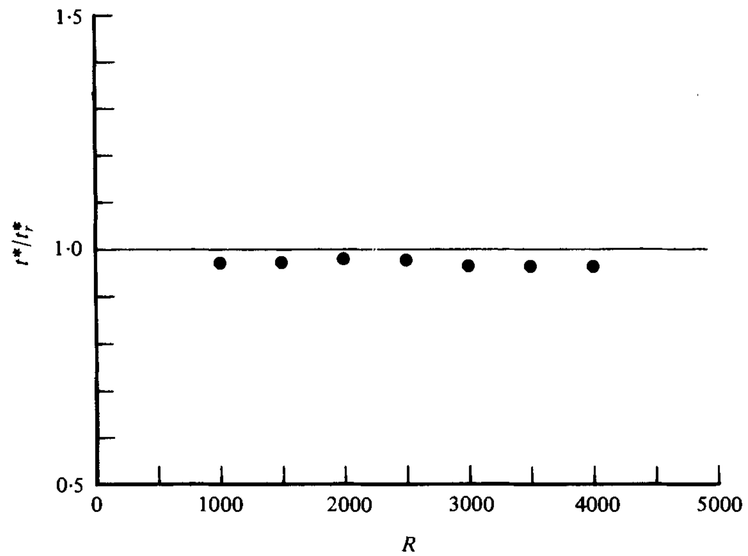

FIGURE 1. The ratio of the time at which the harmonic attains its maximum to the time predicted by linear theory (assuming perfect phase-locking) is plotted as a function of Reynolds number when $\alpha = 1$. The actual (computed) time is less than the predicted linear theory time because the real frequency of the harmonic is not exactly twice that of the primary.

and thus A_2 grows secularly in t for short times and attains a maximum at

$$t^*_r = \frac{\ln(-2\omega_{1i}) - \ln(-\omega_{2i})}{-2\omega_{1i} + \omega_{2i}}. \tag{20}$$

As the modes are not exactly phase-locked, we would expect the actual maximum to occur at $t^* < t^*_r$. This behaviour is verified in figure 1 by a plot of t^*/t^*_r at $\alpha = 1$ for various Reynolds numbers. The maximum deviation between (20) and our direct simulations is $-3\,\%$.

Next, we study finite-amplitude disturbances predicted to be dangerous by the method of false problems. Davey & Nguyen (1971) find that the two disturbances tested above at very small amplitude (see Table 1) have threshold (unstable equilibrium) energies (19) of $E \simeq 0{\cdot}003$. The method of Itoh (1977) as applied by Davey (1978) indicates that the *centre* mode should decay at finite amplitude, however it too predicts a small-amplitude equilibrium state for the *wall* mode. To test these theoretical results, the same series of runs reported in table 1 were repeated except that the axial and radial resolution was increased, the time integration was taken to a final time of $T = 20$ rather than $T = 10$, and the initial energies of the disturbance were taken to be 0·01. The results for the wall mode and centre mode are shown in figures 2 and 3 respectively, as plots of the logarithm of the primary and secondary energies as a function of time. There is apparently no evidence of equilibria. Runs at lower and higher initial energies (e.g. $E \simeq 0{\cdot}04$ or amplitudes of order 20 %) decay in a similar manner. Note that the normalization of E chosen in (19) implies that centre modes have larger initial velocity amplitudes than wall modes with the same energy.

The lack of equilibria reported above does not preclude their existence for other Reynolds-number/wavenumber combinations. However, in a variety of runs, we

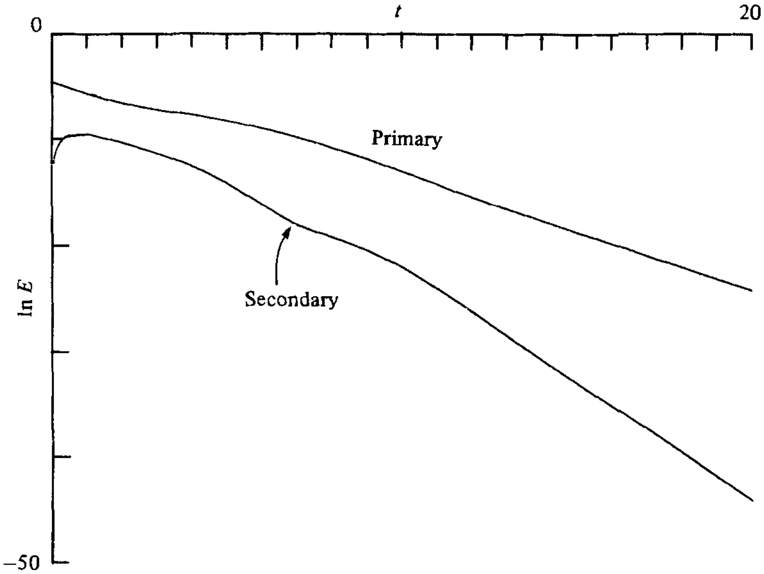

FIGURE 2. Decay of a wall mode at $R = 1600$, $\alpha = 5{\cdot}8$ from an initial energy ($E = 0{\cdot}01$) larger than the equilibrium value predicted by the method of false problems. Higher energy disturbances also decay. Here E is the energy of the disturbance relative to the mean flow [defined in (19)]. Also, $N = 8$ and $P = 64$ in (4)–(5). The accuracy of this and other runs was tested by changing N, P and the time step Δt.

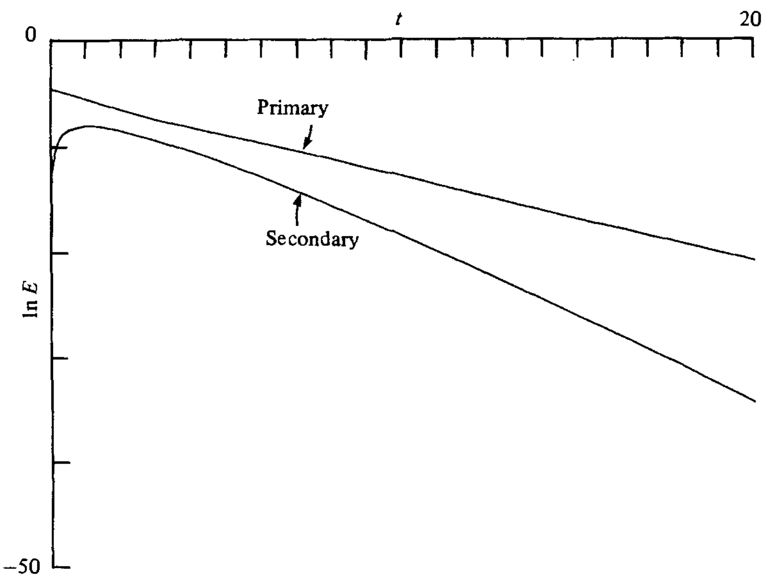

FIGURE 3. Decay of a centre mode at $R = 500$, $\alpha = 6{\cdot}2$ from an initial energy ($E = 0{\cdot}01$) larger than the equilibrium value predicted by perturbation theory. Here $N = 8$ and $P = 32$ in (4)–(5).

have found no finite-amplitude steady-states. The results of a typical run at $R = 4000$ $\alpha = 1{\cdot}0$, $\omega = 0{\cdot}3783 - i\,0{\cdot}1025$, are plotted in figure 4. From figure 4 we infer that the disturbance at $R = 4000$ decays in a time very short compared to a diffusive time scale, and is therefore consistent with the absence of equilibria (Orszag & Patera 1980).

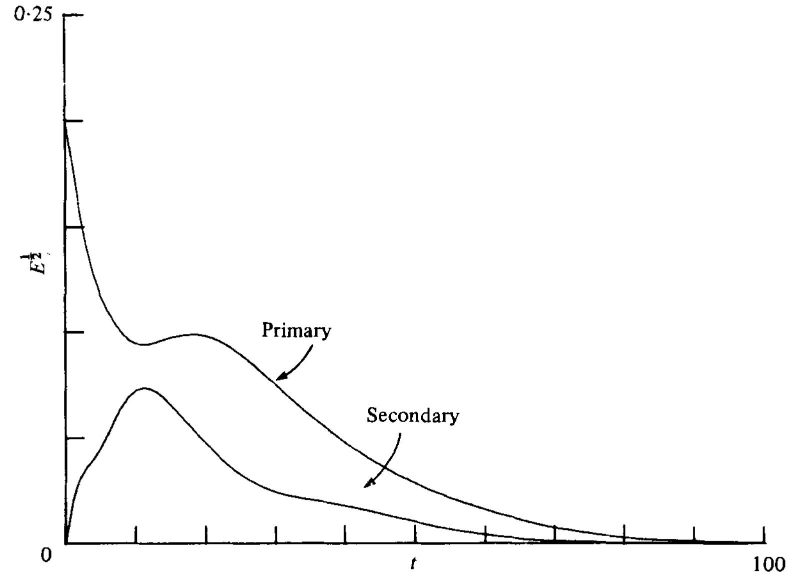

FIGURE 4. Decay of a wall mode at $R = 4000$, $\alpha = 1$. The decay occurs on a time scale much shorter than the diffusive scale indicating the absence of equilibria. Here $N = 8$ and $P = 32$ in (4)–(5).

The time scale for decay of finite-amplitude axisymmetric states is central to an understanding of three-dimensional transition. The three-dimensional instability mechanism leading to transition in plane Poiseuille and Couette flows (Orszag & Patera 1980) develops on a time scale significantly shorter than the time scale on which two-dimensional perturbations of these flows decay. This three-dimensional instability of planar channel flow is also relevant to transition in pipe flow. The behaviour of non-axisymmetric disturbances to decaying axisymmetric states will be considered in a later paper.

Our results indicate that the method of false problems is not a valid procedure for investigating finite-amplitude axisymmetric perturbations to pipe flow. We do not attempt a critique of these methods here except to emphasize a point made by Herbert (1977). Herbert commented that the retention of only the first term in the amplitude expansion of the frequency without knowing the convergence properties of the series can lead to incorrect conclusions, especially in cases (such as pipe flow and plane Couette flow) where there is no linear neutral curve. The radius of convergence of the amplitude expansion may simply be too small to predict equilibria. For example, numerical simulations of plane Couette flow (Orszag & Kells 1980; Patera & Orszag 1980) do not confirm the existence of two-dimensional equilibria predicted by Davey & Nguyen (1971) on the basis of amplitude expansions. The direct iteration procedure of Herbert (1977) bypasses this problem and can predict the existence of equilibria as well as their threshold energy. However, a limited survey of the available phase space has not yet yielded any finite-amplitude solutions. We suspect there are none.

This work was supported by the Office of Naval Research under Contract N00014-77-C-0138 and the National Aeronautics and Space Administration under Contract no. NAS1-15894.

REFERENCES

DAVEY, A. 1978 On Itoh's finite amplitude stability theory for pipe flow. *J. Fluid Mech.* **86**, 695–703.

DAVEY, A. & DRAZIN, P. G. 1969 The stability of Poiseuille flow in a pipe. *J. Fluid Mech.* **36**, 209–218.

DAVEY, A. & NGUYEN, H. P. F. 1971 Finite-amplitude stability of pipe flow. *J. Fluid Mech.* **45**, 701–720.

GOTTLIEB, D. & ORSZAG, S. A. 1977 *Numerical Analysis of Spectral Methods: Theory and Applications.* NSF-CBMS Monograph no. 26. Soc. Ind. App. Math., Philadelphia.

HERBERT, T. 1977 Finite amplitude stability of plane parallel flows. In *Laminar-Turbulent Transition, AGARD Conf. Proc.* no. 224, 3-1–3-10.

ITOH, N. 1977 Nonlinear stability of parallel flows with subcritical Reynolds number. Part 2. Stability of pipe Poiseuille flow to finite axisymmetric disturbances. *J. Fluid Mech.* **82**, 469–479.

LESSEN, M., SADLER, S. G. & LIU, T. Y. 1968 Stability of pipe Poiseuille flow. *Phys. Fluids* **11**, 1404–1409.

METCALFE, R. W. & ORSZAG, S. A. 1973 Numerical calculation of the linear stability of pipe flows. *Flow Research Rep.* no. 25, Kent, Washington.

ORSZAG, S. A. 1971 Accurate solution of the Orr–Sommerfeld stability equation. *J. Fluid Mech.* **50**, 689–703.

ORSZAG, S. A. & KELLS, L. C. 1980 Transition to turbulence in plane Poiseuille and plane Couette flow. *J. Fluid Mech.* **96**, 159–205.

ORSZAG, S. A. & PATERA, A. T. 1980 Subcritical transition to turbulence in plane channel flows. *Phys. Rev. Lett.* **45**, 989–992.

PATERA, A. T. & ORSZAG, S. A. 1980 Transition and turbulence in planar channel flows. In *Proc. 7th Int. Conf. on Numerical Methods in Fluid Dynamics* (ed. W. C. Reynolds & R. W. MacCormack), pp. 329–335. Springer.

SALWEN, H., COTTON, F. W. & GROSCH, C. E. 1980 Linear stability of Poiseuille flow in a circular pipe. *J. Fluid Mech.* **98**, 273–284.

SEXL, T. 1927 Zur Stabilitätsfrage der Poiseuilleschen und Couetteschen Strömüng. *Ann. Physik* **83**, 835–848.